Human Molecular Genetics, 2011, Vol. 20, No. 6 **1061–1073**
doi:10.1093/hmg/ddq549
Advance Access published on December 21, 2010

KASH protein Syne-2/Nesprin-2 and SUN proteins SUN1/2 mediate nuclear migration during mammalian retinal development

Juehua Yu[1,†], Kai Lei[1,†], Min Zhou[2], Cheryl M. Craft[3,4,5], Gezhi Xu[2], Tian Xu[1,6], Yuan Zhuang[1,7], Rener Xu[1,*] and Min Han[1,8]

[1]Institute of Developmental Biology and Molecular Medicine, School of Life Science, Fudan University, Shanghai 200433, China, [2]Department of Ophthalmology, Fudan University Eye and ENT Hospital, Shanghai 200031, China, [3]Mary D. Allen Laboratory in Vision Research, Doheny Eye Institute, [4]Department of Ophthalmology and [5]Department of Cell and Neurobiology, Keck School of Medicine of the University of Southern California, Los Angeles, CA 90033, USA, [6]Howard Hughes Medical Institute and Department of Genetics, Yale University School of Medicine, New Haven, CT 06520, USA, [7]Department of Immunology, Duke University Medical Center, Durham, NC 27710, USA and [8]Howard Hughes Medical Institute and Department of MCDB, University of Colorado, Boulder, CO 80309, USA

Received September 15, 2010; Revised November 19, 2010; Accepted December 15, 2010

Nuclear movement relative to cell bodies is a fundamental process during certain aspects of mammalian retinal development. During the generation of photoreceptor cells in the cell division cycle, the nuclei of progenitors oscillate between the apical and basal surfaces of the neuroblastic layer (NBL). This process is termed interkinetic nuclear migration (INM). Furthermore, newly formed photoreceptor cells migrate and form the outer nuclear layer (ONL). In the current study, we demonstrated that a KASH domain-containing protein, Syne-2/Nesprin-2, as well as SUN domain-containing proteins, SUN1 and SUN2, play critical roles during INM and photoreceptor cell migration in the mouse retina. A deletion mutation of *Syne-2/Nesprin-2* or double mutations of *Sun1* and *Sun2* caused severe reduction of the thickness of the ONL, mislocalization of photoreceptor nuclei and profound electrophysiological dysfunction of the retina characterized by a reduction of a- and b-wave amplitudes. We also provide evidence that Syne-2/Nesprin-2 forms complexes with either SUN1 or SUN2 at the nuclear envelope to connect the nucleus with dynein/dynactin and kinesin molecular motors during the nuclear migrations in the retina. These key retinal developmental signaling results will advance our understanding of the mechanism of nuclear migration in the mammalian retina.

INTRODUCTION

The mammalian retina is a highly organized structure that functions physiologically as an external sensor to the central nervous systems. Proper retinal development is critical for the establishment and maintenance of vision circuits. The mammalian retina is comprised of three distinct cell body layers: the outer nuclear layer (ONL), inner nuclear layer (INL) and ganglion cell layer (GCL), separated by the outer (OPL) and inner plexiform layers (IPL), respectively (1). Within these three cell body layers, there are six cell types: photoreceptors in the ONL, bipolar cells, horizontal cells and amacrine cells in the INL, ganglion cells in the GCL, and Müller cells that are a major glia cell type in all three layers (2–6).

Mammalian retinal development involves properly timed cell proliferation, differentiation and migration. Recent studies have revealed at least two kinds of nuclear activities at the proliferative and post-mitotic phases of retinal development (7). Interkinetic nuclear migration (INM) is a process by which the nuclei of retinal progenitor cells (RPCs) oscillate from the apical to basal surfaces (or central to peripheral)

*To whom correspondence should be addressed. Tel: +1 862165642111; Fax: +1 862165643770; Email: rener_xu@fudan.edu.cn
†These authors contributed equally to this work.

of the neuroblastic layer (NBL). Interestingly, the INM occurs in coordination with the progression of the cell cycle; nuclei at the M phase are located at the apical surface, whereas the nuclei at G1-, S- and G2-phases are located at more basal locations (8). Following the exit from the cell cycle, some neuronal precursors migrate to their appropriate positions (7).

The development of mouse retinal photoreceptors takes place in a well-organized temporal sequence. Both rod and cone cell differentiation and synaptogenesis occur postnatally (2–6). Rod photoreceptors have been observed to have a specific nuclear movement during early development (4). Around the fifth postnatal day (P5), when the OPL first appears, a large proportion of rod nuclei are located on the inner side of this layer. Those nuclei will then move through the newly formed OPL and into the ONL. Although this rod photoreceptor nuclear migration pattern was observed decades ago, the underlying molecular and cellular mechanisms remain enigmatic. Moreover, cone cell nuclei also undergo a nuclear migration process during maturation (9). Only 3–5% of the photoreceptors are cone cells in the ONL of the mouse retina (10–12). At the neonatal stage in mice, the cone cells are located just beneath the retinal pigment epithelium of the retina. These cone nuclei then scatter throughout the ONL between P4 and P11. At P12, the cone cells align their cell bodies in the outer surface of the ONL. However, the migration of cone nuclei has not been analyzed by mutagenesis studies in mammals.

KASH domain-containing proteins (KASH proteins) have a conserved protein motif of 60 residues (KASH domain) in their C-terminal end that commonly spans the outer nuclear membrane, which is critical to the interaction between the KASH protein and the conserved inner nuclear membrane SUN domain-containing proteins (SUN proteins) at the nuclear envelope (NE) (13). SUN proteins are necessary for the localization of the KASH proteins to the NE in *Caenorhabditis elegans*, *Drosophila*, mice and tissue cultured cells (14–23). Recently, the KASH and/or SUN proteins have been implicated to be involved in retina photoreceptor nuclear migration and positioning both in flies and in zebrafish. In *Drosophila*, loss of function of either the KASH gene, *klarsicht*, or the SUN gene, *klaroid*, leads to a failure in nuclear migration of photoreceptors during eye development (17,24). In zebrafish, overexpression of a truncated form of Syne2a in the retina also results in abnormal INM and the misplacement of photoreceptor nuclei (25,26).

Mammalian KASH and/or SUN proteins have been extensively studied in gametogenesis, myogenesis and neurogenesis using mouse genetic approaches (14,16,27–30). However, the functions of KASH and SUN proteins during mammalian retinal development are unknown. In this study, we explored the roles of two KASH proteins, Syne-1 (also known as Nesprin-1) and Syne-2 (also known as Nesprin-2), and two SUN proteins, SUN1 and SUN2, in nuclear migration during retinal development in mice. Our results indicate that the KASH protein, Syne-2, and the two SUN proteins mediate nuclear migration of the photoreceptor cells through bridging microtubules with molecular motors to the nuclei.

RESULTS

Deletion of the Syne-2 KASH domain leads to thickness reduction of the ONL of the retina and nuclear mislocalization

To investigate the potential roles of KASH proteins, Syne-1/Nesprin-1 and Syne-2/Nesprin-2, during mouse retinal development, we examined the eyes of adult mice with a KASH domain deletion in either Syne-1 (*Syne-1*$^{-/-}$) or Syne-2 (*Syne-2*$^{-/-}$) (31). The overall structures of these mutant eyes were similar to those of wild-type controls (data not shown). However, the cross-sections of the retina of different genotypes reveal that the ONL of *Syne-2*$^{-/-}$ retinas was visibly thinner (23 μm on average) than that of controls (39 μm on average) (Fig. 1A, B and G). Meanwhile, a group of hematoxylin and eosin (H&E)-stained nuclei, which had similar levels of H&E staining to the nuclei within the ONL, were mislocalized in the OPL and the INL (Fig. 1A and B). Unlike the *Syne-2*$^{-/-}$ retina, the retinal laminar structure was normal in both *Syne-1*$^{-/-}$ and *Syne-1*$^{-/-}$ *Syne-2*$^{+/-}$ genotypes (Fig. 1C and data not shown). We further examined the expression pattern of Syne-1 and Syne-2 in the retina. Syne-1 was undetectable in the retina from embryonic day (E) 18.5 to P9 (Supplementary Material, Fig. S1A–C″), but expression was detectable in the outer segment (OS) of photoreceptors in adults (Supplementary Material, Fig. S1D–D″). Interestingly, the signal of Syne-1 was still detectable with similar intensity in *Syne-1*$^{-/-}$ mice (data not shown), suggesting that the antibody against Syne-1 recognizes a Syne-1 isoform without the KASH domain. Syne-2 was highly expressed on the NE in the mouse retina during development (Supplementary Material, Fig. S1E–H″). From E18.5 to P5, Syne-2 was expressed in both the NBL and GCL. After P5, when the OPL began to appear, the level of Syne-2 in the ONL decreased. After P9, it was highly expressed on the NE of a small number of cells lying within the outer leaflet of the ONL. Meanwhile, the expression pattern of Syne-2 in INL and GCL cells remained unchanged. Because the *Syne-1*$^{-/-}$ *Syne-2*$^{-/-}$ mice died shortly after birth (14,31), we examined only their retinas at E18.5. As shown in Supplementary Material, Figure S2A and B, the retinas of *Syne-1*$^{-/-}$*Syne-2*$^{-/-}$ mice are similar to those of their littermate *Syne-1*$^{+/-}$ *Syne-2*$^{-/-}$ mice at E18.5, supporting the idea that Syne-2, but not Syne-1, plays a major role in retina development.

We further analyzed the *Syne-2*$^{-/-}$ mice to determine the stage at which the thinning of the ONL occurred (Fig. 2). We found that, at the neonatal stages and P3, there were no obvious differences in the overall retina structures between *Syne-2*$^{-/-}$ mice and their wild-type or heterozygous littermates (Fig. 2A, B, F and G). At P5, the OPL began to appear in wild-type mice (Fig. 2D) (7,32), but not in *Syne-2*$^{-/-}$ mice (Fig. 2H). At P9 and P14, the thickness of the ONL in *Syne-2*$^{-/-}$ mice was significantly reduced (Fig. 2D and E, and I and J). These results suggest that Syne-2 is required during retinal ONL formation.

SUN1 and SUN2 have partially redundant roles during ONL development

The observation that KASH domain-containing Syne-2 is required for proper retinal development suggests that a

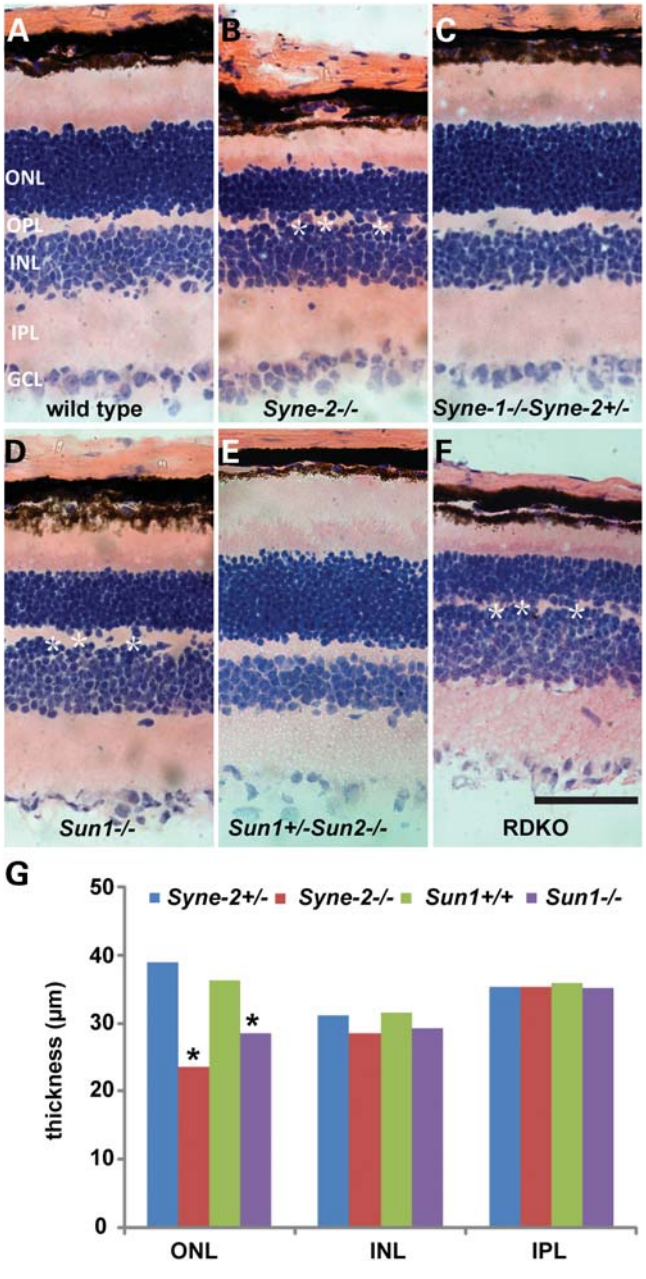

Figure 1. The retinas of *Syne-2*$^{-/-}$, *Sun1*$^{-/-}$ and transgenic RDKO mice display a significant reduction in ONL thickness and nuclear mislocalization. (**A**–**F**) Representative images of H&E-stained retinal sections from 6-week-old mice of the indicated genotypes. In *Syne-2*$^{-/-}$ (B), *Sun1*$^{-/-}$ (D) and RDKO (F) mice, the ONL is thinner than that of wild-type (A), *Syne-1*$^{-/-}$*Syne-2*$^{+/-}$ (C) and *Sun1*$^{+/-}$*Sun2*$^{-/-}$ mice (E). Other structures such as the OPL, INL, IPL and GCL are similar in mice of different genotypes. Asterisks indicate the mislocalized nuclei in *Syne-2*$^{-/-}$, *Sun1*$^{-/-}$ and RDKO mice. (**G**) Histogram showing statistical data of the layer thickness of the ONL, INL and IPL in retina sections of *Syne-2*$^{+/-}$, *Sun1*$^{+/+}$, *Syne-2*$^{-/-}$ and *Sun1*$^{-/-}$mice. $n > 3$ for each genotype. $P < 0.05$. Asterisks denote significant difference of the ONL thickness between mutant mice (*Syne-2*$^{-/-}$ and *Sun1*$^{-/-}$) and the indicated control mice (*Syne-2*$^{+/-}$ and *Sun1*$^{+/+}$). The scale bar is 50 μm.

Syne-2-involved KASH–SUN NE complex may play a critical role in nuclear positioning during ONL development. We thus investigated the potential roles of SUN1 and SUN2 during the development of retina ONL.

The overall structures of eyes of adult *Sun1*$^{-/-}$ and *Sun2*$^{-/-}$ mice were similar to those of wild-type mice (data not shown). H&E-stained cross-sections showed that the thickness of the ONL was reduced in *Sun1*$^{-/-}$ mice (Fig. 1D and G) but normal in *Sun2*$^{-/-}$ and *Sun1*$^{+/-}$*Sun2*$^{-/-}$ mice (Fig. 1E; data not shown). Shown similarly in *Syne-2*$^{-/-}$ retinas, many nuclei were mislocalized in the OPL and INL in *Sun1*$^{-/-}$ retinas. Furthermore, the ONL of *Sun1*$^{-/-}$ mice was significantly thicker than that of *Syne-2*$^{-/-}$ mice (Fig. 1B and D), suggesting a weaker requirement for *Sun1* than for *Syne-2* in the developmental process.

We also examined the expression patterns of SUN1 and SUN2 in the retina. Similar to the expression patterns of Syne-2, SUN1 and SUN2 were highly expressed on the NE in all the cells from embryonic stage to P5 (Supplementary Material, Fig. S1I–K″ and M–O″). After P9, the overall expression of these two proteins was reduced. However, they were highly expressed on the NE of the cells within the outer leaflet of the ONL (Supplementary Material, Fig. S1L–L″ and P–P″). We also determined that the proper NE localization of Syne-2 in retinas depended on the presence of at least one of the two SUN proteins (Supplementary Material, Fig. S2E). These results indicate that SUN1 and SUN2 have partially redundant roles in recruiting Syne-2 to the NE of retina nuclei for their proper functions and that SUN1 plays a more dominant role than SUN2.

Similar to *Syne-1*$^{-/-}$*Syne-2*$^{-/-}$ mice, *Sun1*$^{-/-}$*Sun2*$^{-/-}$ (double knockout, DKO) mice also died shortly after birth (14,16) and did not display any obvious abnormalities in their retinal structures at E18.5 (Supplementary Material, Fig. S2C and D). To examine the retinas of the DKO mice, we used a transgenic mouse line that expressed the *Sun1* gene driven by the neuron-specific enolase (NSE) promoter (16). The *Sun1*$^{-/-}$*Sun2*$^{-/-}$*NSE::Sun1* [death rescued double knockout (RDKO)] mice were alive at birth, and often survived to adulthood. The ONL of adult RDKO mice was visibly thinner than that of *Sun1*$^{-/-}$ mice (Fig. 1F) and similar to that of *Syne-2*$^{-/-}$ mice, which is consistent with the lack of the expression of the *NSE::Sun1* transgene in the retina (data not shown). This result further supports our hypothesis that SUN1 and SUN2 function redundantly in recruiting Syne-2 to the NE for the proper function in the retina.

Consistent with the above observation, we also noted that the progression of the retinal defects in *Sun1*$^{-/-}$ mice closely resembled that in *Syne-2*$^{-/-}$ mice (Fig. 2K–O).

Syne-2$^{-/-}$ and *Sun1*$^{-/-}$ mice exhibit excessive apoptosis in the retina

In the ONL of mouse retinas, 95–97% of photoreceptor cells are rod cells (5). Therefore, the reduction of the thickness of the ONL described above could be attributed mainly to the loss of rod cells. By immunologically staining the rod cells with an antibody directed to rhodopsin, we found significantly fewer rod cells in the ONL of both *Syne-2*$^{-/-}$ (6.5 ± 0.6 rows) and *Sun1*$^{-/-}$ (9.0 ± 1.0 rows) retinas than in that of wild-type retinas (12.0 ± 0.5 rows) (Fig. 3A; data not shown). The reduction of immunopositive rhodopsin-staining rod cells in *Sun1*$^{-/-}$ mice was slightly weaker than that in *Syne-2*$^{-/-}$ mice, which is consistent with the H&E staining results shown

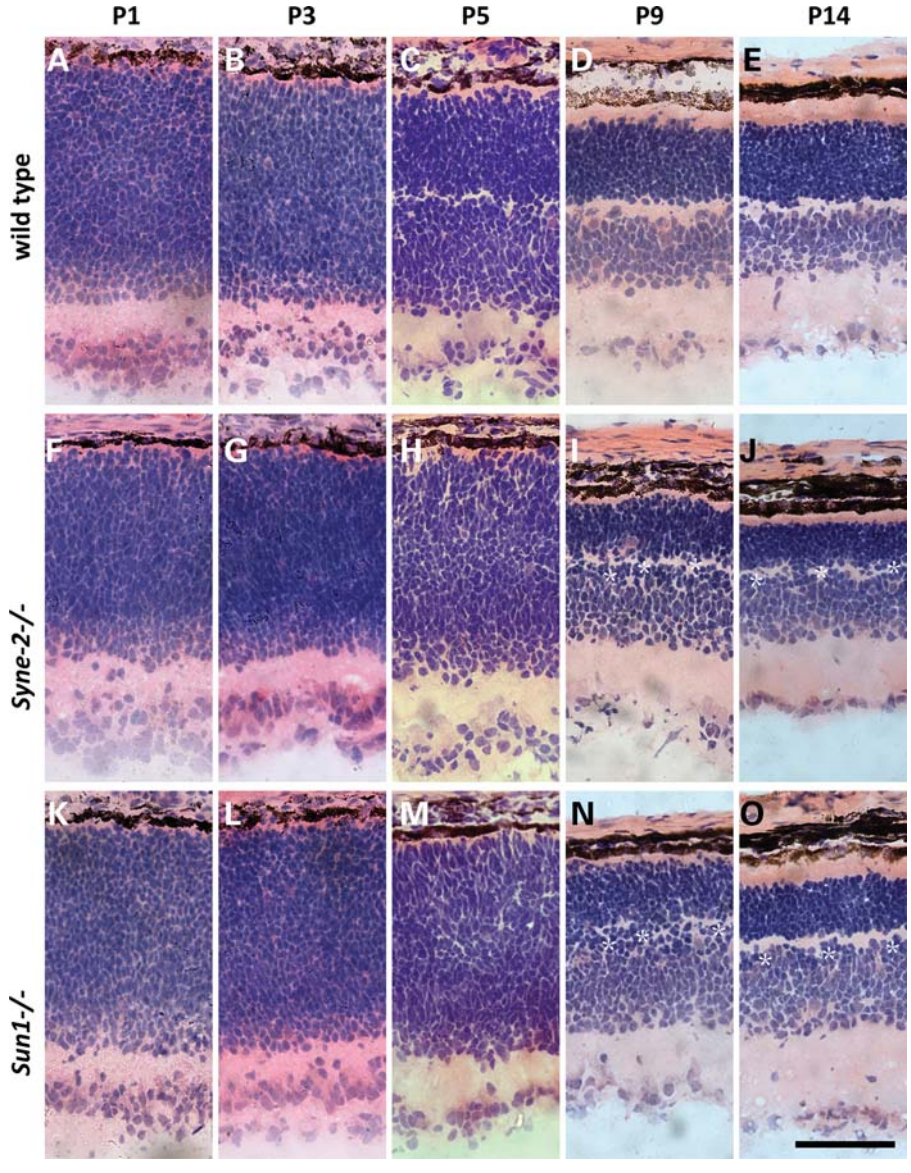

Figure 2. The ONL defects occur in early retinal development of *Syne-2*$^{-/-}$ and *Sun1*$^{-/-}$ mice. Representative images of H&E-stained retinal sections from wild-type (**A–E**), *Syne-2*$^{-/-}$ (**F–J**) and *Sun1*$^{-/-}$ (**K–O**) mice. At P5, layer formation is delayed in the two mutant mice (comparing H and M with C). At P9, the thickness of the ONL in the mutant mice is significantly reduced (comparing I and N with D). Asterisks denote mislocalized nuclei. The scale bar is 50 μm.

in Figure 1. During postnatal development of the retina, both cell proliferation and cell death contribute to the normal development for the generation and maintenance of the appropriate number of photoreceptor cells (4). Thus, an apoptotic TUNEL assay was carried out to analyze the progression of cell death in these mouse mutants at multiple developmental stages. At P3, elevated apoptotic signals were detected in *Syne-2*$^{-/-}$ and *Sun1*$^{-/-}$ retinas (Fig. 3B), and similar results were also observed at P5 in *Syne-2*$^{-/-}$ and *Sun1*$^{-/-}$ retinas (Fig. 3B). As expected, no significant detectable apoptotic signal was detected in 6-week-old adult mice. These results are consistent with our observations of the thickness reduction of the ONL in *Syne-2*$^{-/-}$ and *Sun1*$^{-/-}$ mice, indicating that Syne-2 and SUN1 are involved in an early retinal developmental stage and the loss of function of these proteins eventually leads to an increase in cell death linked to apoptosis.

INM is impaired in the retinas of *Syne-2*$^{-/-}$ and *Sun1*$^{-/-}$*Sun2*$^{-/-}$ mice

During RPC proliferation, the nuclei change their positions within the cell as they progress through the cell cycle (INM). Therefore, we suspected that Syne-2, SUN1 and SUN2 may regulate cell number by influencing INM. To assess this hypothesis, we first performed immunofluorescent (IF) staining using anti-phospho-histone H3 (pH3) and anti-Ki67 antibodies in the retina sections of *Syne-2*$^{-/-}$, *Sun1*$^{-/-}$ and *Sun1/2 DKO* mice at E18.5. Although anti-Ki67 IF failed to detect any obvious reductions of the number of proliferative cells in *Syne-2*$^{-/-}$, *Sun1*$^{-/-}$ and *Sun1/2 DKO* retina, a few anti-pH3-positive mitotic cells were sparsely located within the NBL in both *Syne-2*$^{-/-}$ and *Sun1/2 DKO* retinas (Fig. 3C), indicating a potential

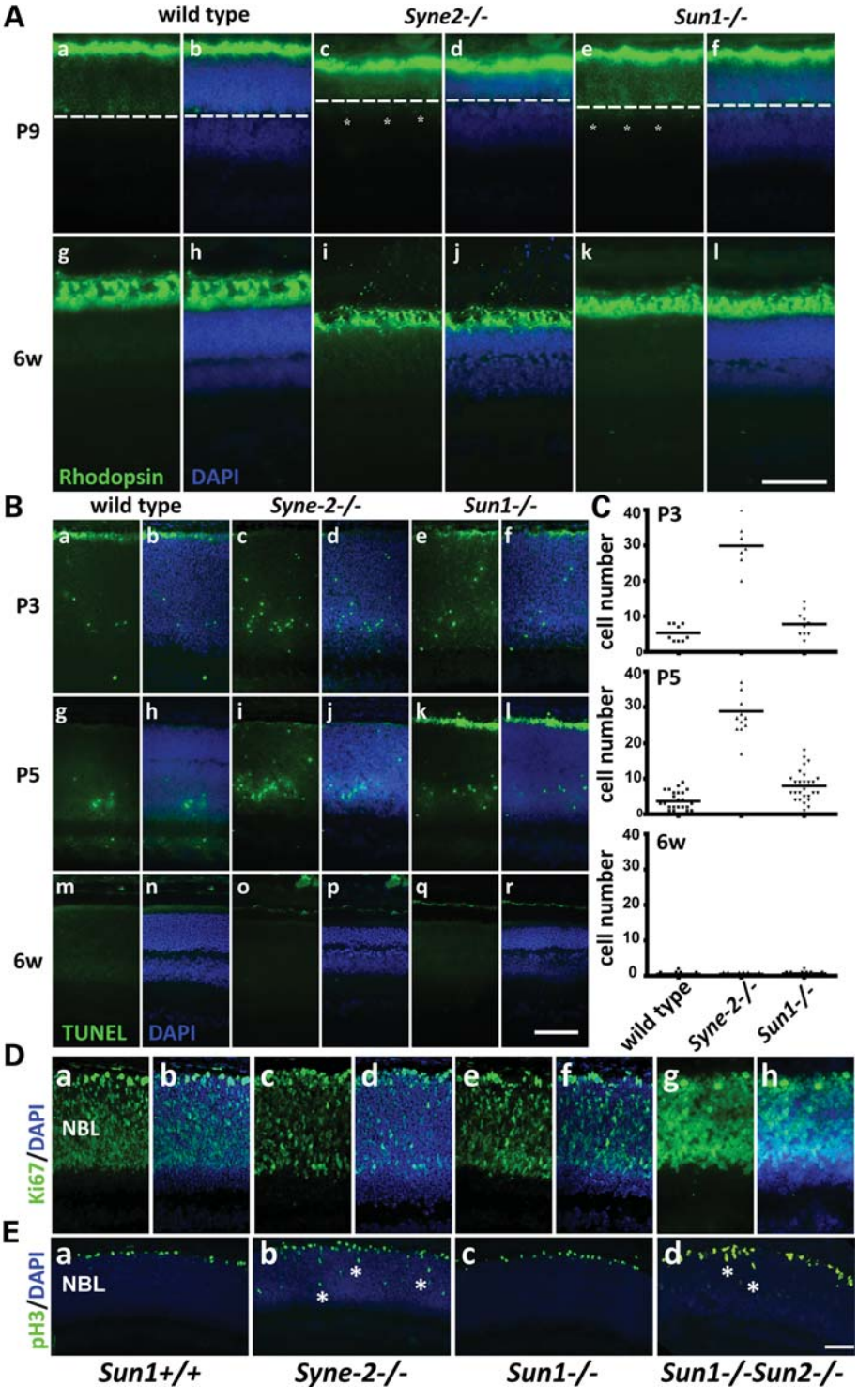

Figure 3. Syne-2 KASH domain deletion or SUN1/2 DKO leads to excessive apoptosis, abnormal INM and rod cell nuclei reduction in the retinas. (**A**) Representative fluorescent images of the anti-rhodopsin staining (green) showing the rod cell loss in *Syne-2*$^{-/-}$ and *Sun1*$^{-/-}$ retinas of mice at the ages of P9 and 6 weeks (6w). The asterisks mark the mislocalized rod cells. (**B**) Representative TUNEL-stained images showing more TUNEL-positive cells (green) in *Syne-2*$^{-/-}$ and *Sun1*$^{-/-}$ retinas than in wild-type retinas at the ages of P3 and P5. The TUNEL signal is undetectable in the retinas of each genotype at the age of 6 weeks. (**C**) Statistical plots showing the average number of TUNEL-positive cells in the retinas of wild-type, *Syne-2*$^{-/-}$ and *Sun1*$^{-/-}$ mice at the ages of P3, P5 and 6 weeks. $P < 0.05$. For each group, the data were collected from images of more than three mice. (**D**) Representative fluorescent images of the anti-Ki67 staining (green) showing similar levels of cell proliferation in wild-type, *Syne-2*$^{-/-}$, *Sun1*$^{-/-}$ and *Sun1*$^{-/-}$ *Sun2*$^{-/-}$ retinas. (**E**) Representative fluorescent images of the anti-pH3 staining (green) showing M-phase cells are mislocalized (asterisks) in *Syne-2*$^{-/-}$ and *Sun1*$^{-/-}$*Sun2*$^{-/-}$ retinas. The scale bar is 50 μm.

defect in INM of these nuclei. These data suggest Syne-2 and SUN1/2 play a critical developmental role in INM during retinal cell proliferation, which is similar to their functional role in the development of the brain cortex (14). To further uncover the roles of Syne-2 in INM during retinal cell proliferation, we performed injection of BrdU (5-bromo-2-deoxyuridine) into *Syne-2*$^{-/-}$ retinas and IF staining at different time points post-injection (Fig. 4). The IF staining results showed that the difference between *Syne-2*$^{-/-}$ and *Syne-2*$^{+/-}$ retinas appeared ∼9 h post-injection of BrdU. Eighteen hours after injection, more BrdU-positive nuclei could be detected along the outer border of NBL in the *Syne-2*$^{-/-}$ retinas than those in control retinas (Fig. 4), indicating that those accumulated nuclei failed to migrate after cell division (disruption of INM). To address the question of whether the INM defect influences cell cycle progression, we examined the cell cycle distribution of progenitors in *Syne-2*$^{-/-}$ and *Syne-2*$^{+/-}$ retinas after 18 h BrdU exposure using flow cytometry (Supplementary Material, Fig. S3). Consistent with the observations described earlier, including the increased apoptotic signals in *Syne-2*$^{-/-}$ retinas, the percentage of BrdU-positive cells in *Syne-2*$^{-/-}$ retinas was slightly, but significantly, reduced. In addition, although there was no significant change in cell populations at G0/G1 and G2/M phases, cell number at S-phase is slightly increased in the *Syne2*$^{-/-}$ retina (Supplementary Material, Fig. S3). These data are consistent with the idea that Syne-2 and SUN1/2 play critical roles in INM and retinal cell proliferation.

Nuclear migration of rod cell is disturbed in *Syne-2*$^{-/-}$ and *Sun1*$^{-/-}$ mice

As described above (Fig. 1), *Syne-2*$^{-/-}$ and *Sun1*$^{-/-}$ mice also exhibit a nuclear mislocalization phenotype in their retinas. To identify the cell type of those mispositioned nuclei, we performed IF staining on the sections of the retinal samples from *Syne-2*$^{-/-}$ and *Sun1*$^{-/-}$ mice using distinct retinal cellular markers. By staining with an anti-PKCα antibody specific to rod bipolar cells (Supplementary Material, Fig. S4), we excluded the possibility that these mislocalized nuclei were rod bipolar cells. Furthermore, we found that overexposure of the anti-rhodopsin IF signals in P9 mice revealed an unusual localization of rhodopsin proteins in those mislocalized nuclei (Fig. 3A) in both *Syne2*$^{-/-}$ and *Sun1*$^{-/-}$ retinas, indicating that these are rod cell nuclei. In addition, IF staining for Arrestin1 with a mouse monoclonal anti-D9F2 antibody (33,34) also showed that the nuclei associated with rod staining, which are positive for Arrestin1 but negative for cone Arrestin4 (anti-mCAR/LUMIj) (35), were mislocalized in both *Syne-2*$^{-/-}$ and *Sun1*$^{-/-}$ retinas (Fig. 5A). It has been previously reported that the group of rod cells isolated on the inner side of the ONL migrate from the newly formed OPL to the ONL in the retina around P5 (4). Thus, these results indicate that Syne-2 and SUN1 are involved in proper nuclear migration of rod cells. Noticeably, only a small population of rod cell nuclei in *Syne-2*$^{-/-}$ and *Sun1*$^{-/-}$ retinas was observed to be mislocalized in the INL (Figs 1 and 5). It is currently not clear whether these defective rod cells were generated at a late stage during retinal development.

Nuclear migration in cone cells is disrupted in *Syne-2*$^{-/-}$ and *Sun1*$^{-/-}$ mice

Although only 3–5% of the photoreceptor cells in the ONL of mouse retina are cone cells, these cone cells are responsive to brighter light intensity and are vital for both discrimination of colors and high-acuity vision (36). It has been reported that the cone cell nuclei migrate through the ONL and are eventually localized to the outermost of the ONLs (9). We therefore examined the localization of cone cell nuclei in *Syne-2*$^{-/-}$ and *Sun1*$^{-/-}$ retinas by immunohistological staining of the cone from the synapse to their OS with an antibody against the cone Arrestin4 (mCAR/LUMIj) (33,35). We found that although the cone cell nuclei were located along the outer leaflet of the ONL in the wild-type retina, they were displaced to the inner edge of the ONL in *Syne-2*$^{-/-}$ and *Sun1*$^{-/-}$ mice (Fig. 5A). The nuclear migration of cone cells is crucial for their normal maturation (9). Using fluorescein-labeled peanut agglutinin (PNA) staining to highlight the OSs of the cone cells in adult mice, we observed that most of the cone cell OSs were lost in *Syne-2*$^{-/-}$ and RDKO mouse retinas, whereas the cone cell OSs in *Sun1*$^{-/-}$ retinas appeared similar to those in wild-type mice (Fig. 5B). These results indicate that the normal nuclear migration of cone cells is disrupted in *Syne-2*$^{-/-}$ and *Sun1*$^{-/-}$ mice and the severe loss of cone cells in *Syne-2*$^{-/-}$ and RDKO mouse retinas is probably due to defects in early stage proliferation and differentiation of the progenitors, which is consistent with our TUNEL assay data (Fig. 3B). However, these data do not rule out the possibility that some of the cone cell loss is due to cell death occurring in late stages. Analysis by using an early cone cell marker would help address this in future.

In addition, the expression patterns of SUN1 and SUN2 in the ONL of *Syne-2*$^{-/-}$ and *Sun1*$^{-/-}$ retinas were altered. In the adult wild-type mouse retina, these proteins are confined on the NE of a group of cells along the outer leaflet of the ONL (Supplementary Material, Fig. S5A, B, E and F), similar to those cells stained positive for cone Arrestin4, which labels all cone cells (Fig. 5Ac). However, these SUN1- and SUN2-positive nuclei were located close to the inner edge in the retinas of both *Syne-2*$^{-/-}$ and *Sun1*$^{-/-}$ mice (Supplementary Material, Fig. S5C, D, G, H, I and J). These results further support the idea that Syne-2, SUN1 and SUN2 are localized on the NE of cone cells and are required for their proper migration. Intriguingly, mCAR antibody staining did not show the same mislocalization pattern of cone nuclei (Fig. 5; Supplementary Material, Fig. S5), raising the question of whether the mCAR marks a different set of cone cells in the mutant. It would also be interesting to use an early cone cell marker along with SUN1 or mCAR antibody to track the positions of cone nuclei at different postnatal stages.

Electroretinography reveals physiological dysfunctions of *Syne-2*$^{-/-}$ and *Sun1*$^{-/-}$ retinas

To analyze the physiological consequences of the developmental defects in the photoreceptor cells described above, we carried out electroretinography (ERG) experiments on adult *Syne-2*$^{-/-}$ and *Sun1*$^{-/-}$ mice as well as on their

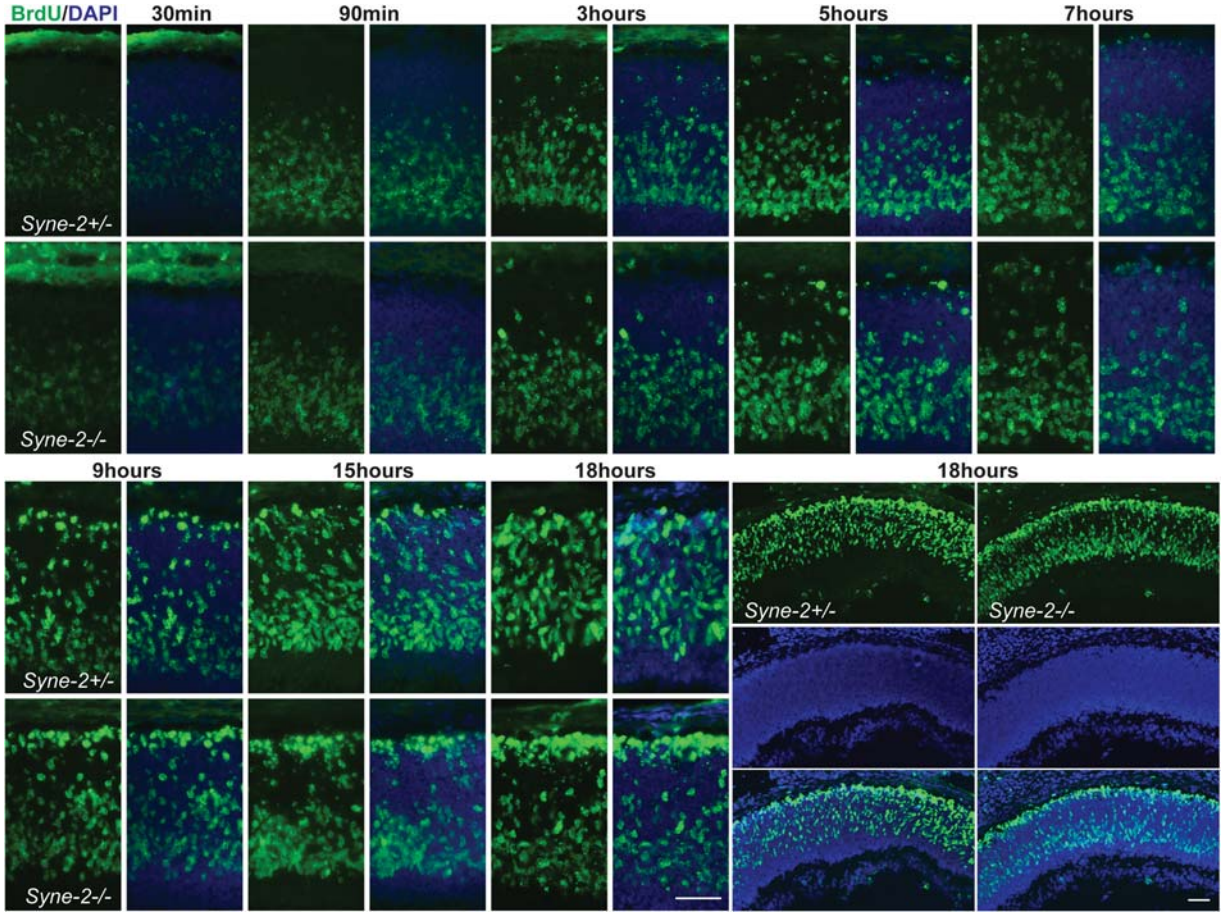

Figure 4. Time-lapse imaging of BrdU-labeled progenitor cells in P3 *Syne-2*$^{-/-}$ retinas. The movement of BrdU-labeled progenitors in retinas. Representative images showing the localization of progenitors in retinas of *Syne-2*$^{+/-}$ and *Syne-2*$^{-/-}$ mice after BrdU labeling at the time points indicated. The scale bar is 50 μm.

littermate controls. Under dark adaptive conditions, the ERG b-wave amplitudes reflect the extracellular potential that primarily arises downstream of the phototransduction signal cascade. By applying light stimuli of higher intensity, the ERG a-wave amplitude can be evoked from both rod and cone photoreceptors (37). Compared with the littermate controls, both a-wave and b-wave amplitudes were significantly lower in *Syne-2*$^{-/-}$ mice (Fig. 6). Interestingly, *Sun1*$^{-/-}$ mice displayed a similar reduction of the a-wave, but no apparent abnormality in the b-wave (Fig. 6), suggesting that *Sun1*$^{-/-}$ mice still have enough viable photoreceptors to form the appropriate synaptic connections with rod and cone bipolar cells. Taken together, these altered ERG responses are consistent with the structural abnormalities that affect the retinal circuitry in both *Syne-2*$^{-/-}$ and *Sun1*$^{-/-}$ mice.

Syne-2 probably mediates nuclear migration in the retina through a connection with both dynein/dynactin and kinesin complexes

The minus-end microtubule molecular motors, dynein/dynactin complex transport its cargo over long distances along the microtubule network (38). Previous studies using other systems have described the interactions between KASH proteins and dynein/dynactin complexes, as well as kinesin complexes, for various nuclear migration functions (14,22,25,26,39–43). We tested the hypothesis that Syne-2 bridges the nucleus to the microtubules for retinal nuclear migration and positioning by interacting with these molecular motor complexes. Using co-immunoprecipitation (co-IP), we showed that both the dynein intermediate chain (IC) and a subunit of dynactin complex, p150, could be immunologically pulled down by the anti-Syne-2 antibody from the retina lysate (Fig. 6A and B). In addition, we also showed that the anti-Syne-2 antibody could pull down the kinesin (KIF5B) from the retina lysate (Fig. 7C), consistent with Syne-2 interacting with kinesin for proper INM function during retinal development. Furthermore, IF staining suggests that Syne-2 co-localized with dynein IC, dynactin p150 and KIF5B on the NE of photoreceptor cells (Fig. 7D–F), although we have not been able to determine whether the NE localization of these motor proteins is dependent on Syne-2. These results are consistent with Syne-2 interacting with both dynein/dynactin and kinesin complexes for INM and nuclear migration of photoreceptors during retinal development. However, because the antibodies we used for co-IP are not specific to migrating cells, the co-IP results do not exclude the possibility that the observed interaction occurred in non-migrating cells.

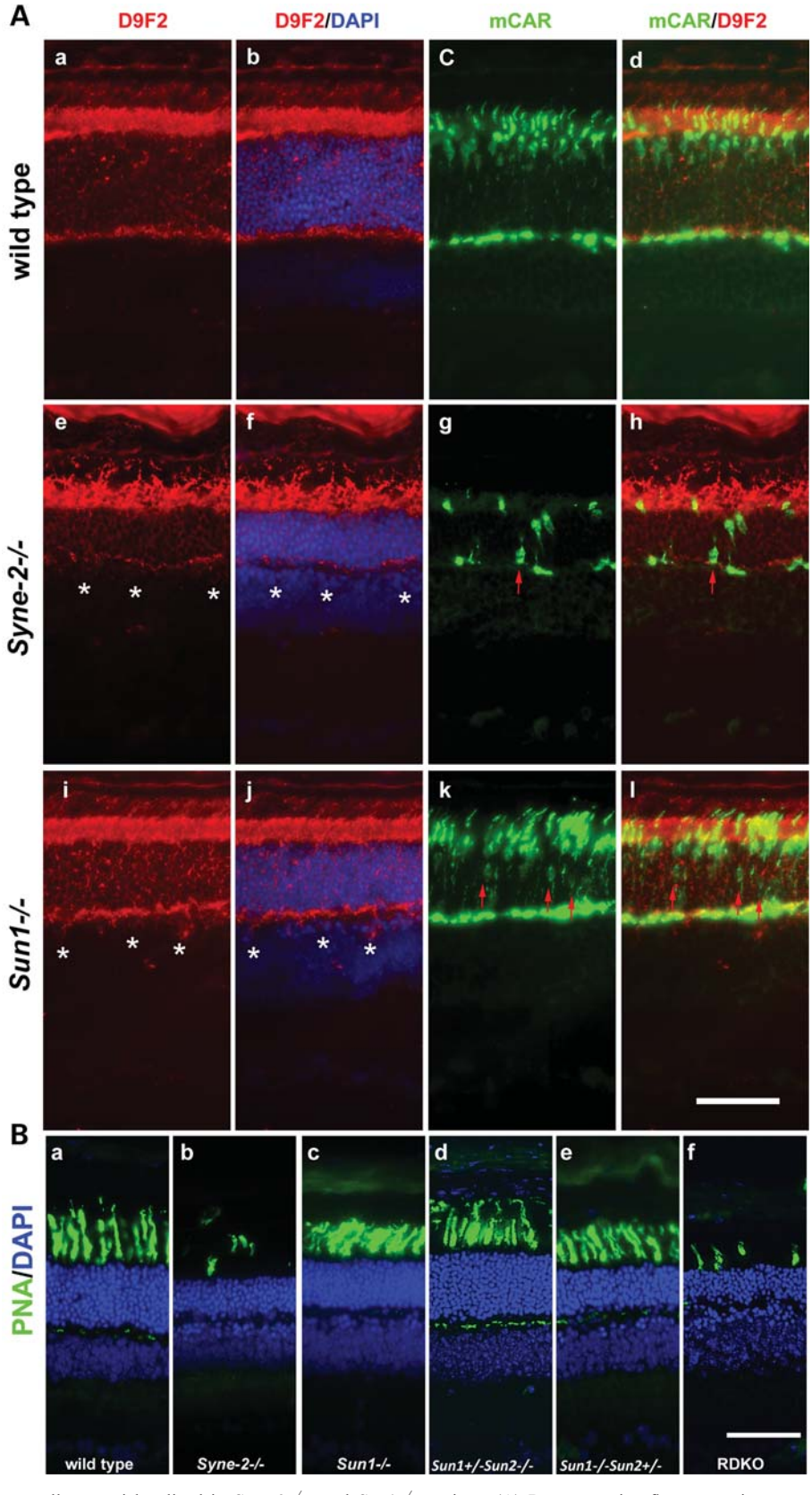

Figure 5. The nuclei of cone cells are mislocalized in *Syne-2*$^{-/-}$ and *Sun1*$^{-/-}$ retinas. (**A**) Representative fluorescent images of anti-mCAR/LUMIj (cone Arrestin4) (green) and anti-D9F2 (Arrestin1) staining (red), showing the cone cells (green) and rod cells (red) in retinal sections from 8-week-old mice of the indicated genotypes. Both cone cells (red arrows) and rod cells (white asterisks) are mislocalized in the mutants. The number of cone cells was also noticeably reduced in *Syne-2*$^{-/-}$ mice. The scale bar is 30 μm. (**B**) Representative images of the anti-PNA staining (green) in retinal sections from 8-week-old mice showing that the number of cone cell OSs is dramatically reduced in the *Syne-2*$^{-/-}$ and RDKO retinas. The scale bar is 50 μm.

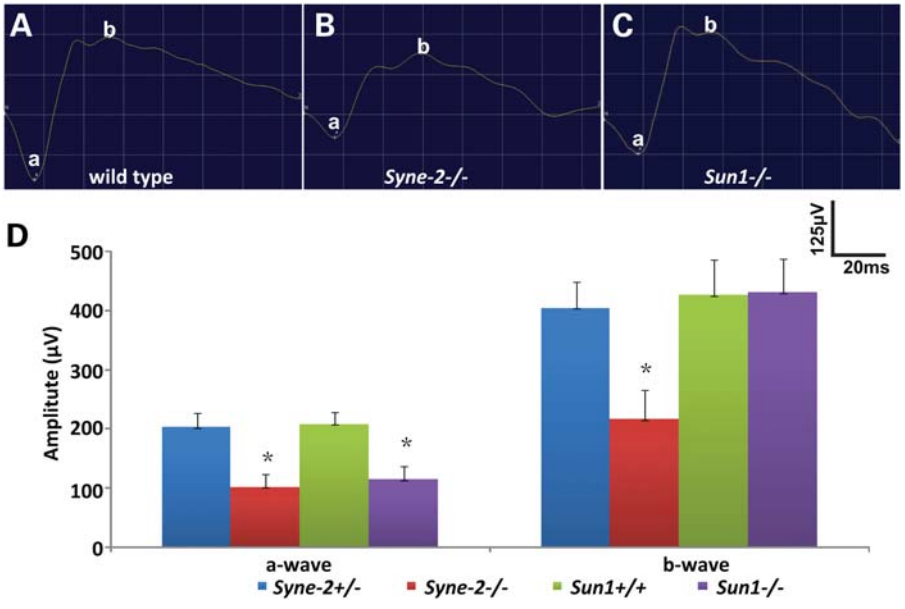

Figure 6. ERG recording shows abnormal physiological function in *Syne-2*$^{-/-}$ and *Sun1*$^{-/-}$ mice. (**A–C**) Representative ERG amplitude curves from wild-type, *Syne-2*$^{-/-}$ and *Sun1*$^{-/-}$ mice. The 'a' and 'b' indicate the a- and b-wave amplitudes, respectively. (**D**) Histogram of statistical analysis showing the amplitude number of a-waves and b-waves in *Syne-2*$^{+/-}$, *Syne-2*$^{-/-}$, *Sun1*$^{+/+}$ and *Sun1*$^{-/-}$ mice at the age of 10–12 weeks; $n \geq 5$ for each genotype; $P < 0.05$.

DISCUSSION

Previous studies have shown that the mammalian KASH and SUN proteins, Syne-1/2 (Nesprin-1/2) and SUN1/2, mediate the nuclear anchorage and migration process in skeletal muscles and the brain (14,16,27,28,31). In this report for the first time, we uncovered the essential modulatory roles of Syne-2 and SUN1/2 in rod and cone nuclear migration in the mouse retina at postnatal developmental stages.

Redundancy and specificity associated with the function of KASH and SUN proteins in mouse development

By analyzing genetic mutants, our previous study builds upon earlier work and establishes the KASH protein pair, Syne-1 and Syne-2, as well as the SUN protein pair, SUN1 and SUN2, to be both structural and functional homologs (14,16,30,31). The fact that postnatal lethality was only observed when we either deleted the KASH domain of both Syne proteins or mutated both SUN proteins indicates clearly that these homologs share critical physiological roles and genetic redundancy, if not the same essential biochemical roles, during development. However, the redundancies of these homologs are clearly not complete. In the case of SUN proteins, the functional differences appear to be due to the differences in expression levels. In some cells, although both proteins share the same function, expression of one protein is insufficient to fully support the appropriate normal function. For example, in skeletal muscle cells, although expression of either SUN1 or SUN2 is sufficient to support the anchorage of non-synaptic nuclei, expression of both is needed to recruit the strikingly high level of Syne-1 onto the NE of synaptic nuclei that appears to be important for their anchorage underneath the neuromuscular junction (16,44). In this current study, we present another scenario. In the retina, SUN1 and SUN2 share common functions as indicated by their redundancy in recruiting Syne-2 to the NE of photoreceptor cells and by the more severe phenotype of *Sun1/2* DKO than that of the single deletion mutant of either gene. However, SUN1 clearly plays a more dominant role (Fig. 1D, E and G), which was not observed in the neuronal function in the mouse brain (14). SUN protein functions during gametogenesis provided an extreme case of non-redundancy; only SUN1 is expressed in meiotic cells to mediate anchorage of telomeres of homologous chromosomes to the NE during meiosis I (16,29,30).

The situation with the two Syne proteins is more complex. In skeletal muscle cells, the nuclear anchorage function only requires Syne-1 (27,31,45). Syne-2 is also expressed in skeletal muscle cells (44, and our unpublished data), but apparently it cannot perform the same anchorage functions since the double deletion mutants did not display a more severe phenotype (31). It is unclear whether the Syne-2 protein expressed in the muscle cells contains the actin-binding domain that has been identified as part of the longer isoform of the protein (13,46,47). In contrast, in some aspects of the neuronal functions in the brain and now in the retina, Syne-2, but not Syne-1, plays a dominant role in mediating neuronal migration and INM (14, and Fig. 3C). Syne-1 is expressed in many of these neuronal cells but not always as an NE-localized protein (14), suggesting that a unique isoform of the protein may be expressed. We provide evidence that Syne-2 interacts with the cytoskeleton microtubule system through binding to both dynein/dynectin and kinesin complexes during neuronal migration and INM in both the retina and the brain (14, and Fig. 7). In contrast, Syne-1 has been proposed to interact with the actin cytoskeleton system by its homology to the nuclear anchorage in *C. elegans* (13,31). Therefore, it is

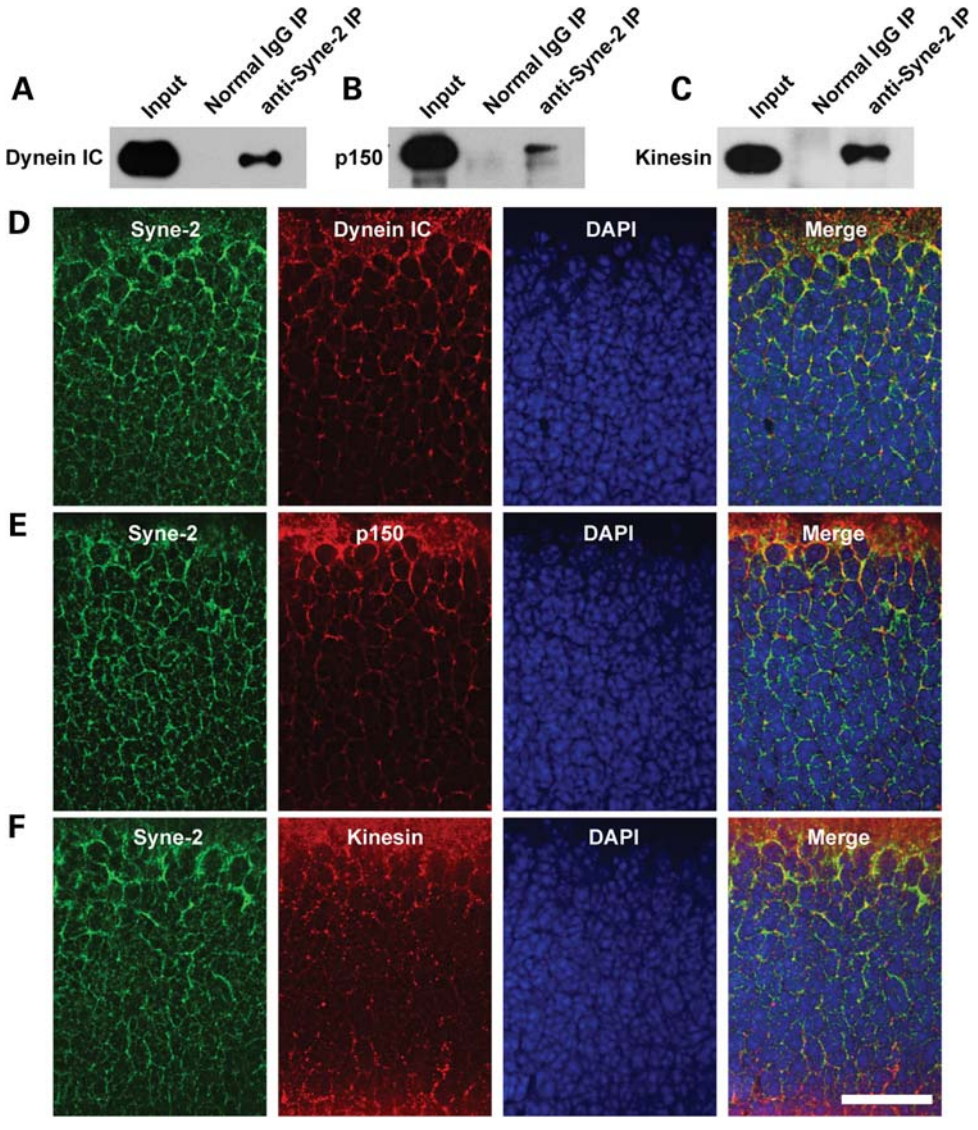

Figure 7. Syne-2 interacts with dynein/dynactin and kinesin complexes. (**A–C**) Immunoblot analysis of SDS–PAGE showing that Syne-2 co-immunoprecipitates with dynein intermediate chain (DIC) (A), p150 (glued) (B) and kinesin (KIF5B) (C) from P5–P9 retinal lysates. (**D–F**) Fluorescent images showing that Syne-2 (green) co-localizes with DIC (D, red), p150 (E, red) and kinesin (KIF5B) (F, red) in P9 retinas. The scale bar is 20 μm.

possible that these two Syne proteins have distinct functions in many tissues. However, it should be noted that we did observe the two Syne proteins acting redundantly for some aspects of the development of brains in mice (14).

Roles of Syne-2 and SUN1/2 in INM of progenitor cells and nuclear migration of photoreceptor cells

Using germline deletion mutations of Syne-2, SUN1 and SUN2, we have observed defects in both INM of proliferating progenitors and nuclear migration of post-mitotic photoreceptor cells. These results raise the question of whether the defects observed in the latter event are the consequence of the defects in the former. When we compared the phenotypes of *Sun1*$^{-/-}$ retinas with those of *Syne-2*$^{-/-}$ or RDKO retinas, we found SUN1 KO affected nuclear migration of post-mitotic photoreceptors but not INM, supporting the notion that the KASH–SUN complexes have roles in the photoreceptor cells that are independent of their roles in INM of the progenitors. Generating conditional KO mice, in which Syne-2 or SUN1/2 are specifically mutated in the photoreceptor cells, would be a more robust approach to address this question.

Earlier reports have suggested that abnormal INM could cause a greater number of progenitors to exit the cell cycle prematurely. For example, in zebrafish, defects in INM are accompanied by the differentiation of more ganglion cells, but fewer bipolar and Müller cells develop (25). However, in our analysis of mouse retinas using anti-PKCα immunological staining, we did not detect a significant reduction of rod bipolar cells in *Syne-2*$^{-/-}$ and *Sun1*$^{-/-}$ mice (Supplementary Material, Fig. S4). In addition, disruption of Syne-2 or SUN1/2 in mice caused the reduction of the thickness of only the ONL, but not that of the INL and GCL

(Fig. 1). This result is also different from the observations made in zebrafish, where defects are also associated with the INL and GCL (25). It is not clear whether the weaker phenotypes observed in mice are the consequence of the functional redundancy provided by additional KASH–SUN complexes.

Syne-2 and SUN1/2 mediate nuclear migration through connecting with dynein, dynactin and kinesin in the mouse retina

Our results demonstrate that the mammalian KASH protein, Syne-2, and SUN proteins, SUN1 and SUN2, are involved in nuclear migration of photoreceptors during mouse retinal development. Previous studies on *Drosophila* have shown that the KASH protein, Klarsicht, and the SUN protein, Klaroid, are involved in photoreceptor nuclear anchorage and migration during eye development (17). Similar findings were obtained in zebrafish, showing that the KASH protein, Syne2a, and dynactin mediate photoreceptor positioning during vertebrate retinal development (26). Our earlier studies in the brain led to a suggestion that Syne-2 interacts with both dynein/dynactin and kinesin complexes during neuronal cell migration and INM in the mouse brain (14). The role of dynein in neuronal migration has been well documented in previous studies (48). The roles of kinesin have been indicated only recently. For example, in a recent report, Kinesin 3 was shown to play a critical role in mediating INM in the mammalian brain (49). Interaction between kinesin and a KASH–SUN complex during nuclear migration in *C. elegans* has also recently been shown and analyzed in detail (50). Therefore, our co-IP data showing interactions of Syne-2 with both kinesin and dynein complexes probably reflect the interactions involved in nuclear migration in the retina.

Recent studies also showed that myosin II is required for the INM both in the zebrafish retina and in the mouse brain (51–53). We found that the non-muscle myosin IIB heavy chain (HC) is co-localized with dynein IC in the mouse retina (Supplementary Material, Fig. S6). Therefore, Syne-2 interaction with myosin for normal functioning in the mouse retina remains to be determined.

MATERIALS AND METHODS

Animals

Mouse breeding and experimental manipulations followed the general guidelines published by the Association for Assessment and Accreditation of Laboratory Animal Care. All mouse strains in this study were generated in our laboratory and maintained on a C57/Bl6- and 129/SVJ-mixed background (16,30,31). All animal-related procedures were reviewed and approved by the Institute of Developmental Biology and Molecular Medicine Institutional Animal Care and Use Committee.

Histological analysis and IF staining

The eyeballs were dissected out and directly embedded in Frozen Section Medium Neg-50 (Richard-Allan Scientific) by immediately freezing them in liquid nitrogen-cooled isopentane. H&E staining was conducted following the method previously described (31).

Eye sections were fixed in 0.4% paraformaldehyde in phosphate-buffered saline (PBS) solution. They were then washed with PBS several times and resuspended in PBS with 0.2% Triton X-100 for 1 h at room temperature. Blocking was performed by incubating the sections at room temperature in PBST (0.2% Triton X-100 in PBS) with 5% normal goat serum for at least 1 h. Samples were then incubated overnight with diluted antibodies in PBST with 5% normal goat serum at 4°C, and then washed three times in PBST. Secondary antibodies, fluorescein isothiocyanate (FITC)-conjugated goat anti-rabbit IgG (Sigma, 1:500) or FITC-conjugated goat anti-mouse IgG (Sigma, 1:200), were used to visualize the protein staining. For DNA visualization, all the samples were washed several times with PBST and stained for 10 min with 4′,6-diamidino-2-phenylindole (DPAI) before they were mounted in anti-fading solution for photographing. The antibodies used in this study were mouse anti-rhodopsin (04886, Sigma, 1:500), mouse anti-PKCα (P5704, Sigma, 1:500), rabbit anti-cone Arrestin4 (mCAR/LUMIj, 1:500) (35), mouse anti-Arrestin1 (D9F2) (generously provided by Larry A. Donoso, 1:20 000), mouse anti-dynein IC (MAB1618, Chemicon, 1:500), mouse anti-p150 (Glued) (610474, BD Bioscience, 1:500), mouse anti-kinesin (KIF5B) (MAB1614, Chemicon, 1:500) and rabbit anti-non-muscle myosin IIB HC (generously provided by Xiaobing Yuan,1:500).

For PNA staining, fixed frozen sections were washed with PBS two to three times, and blocked with the blocking solution (0.5 mg/ml BSA in PBS) for 30 min at room temperature. Fluorescent-labeled PNA (Vector, 1:500) and DAPI (D8417, Sigma, 1:1000) in PBS were then added and incubated for 30 min at room temperature. The sections were washed three times with PBS before they were mounted in anti-fading solution for photographing.

Microscopy

Samples were visualized and photographed with Leica DMRXA2 and DMIRE2 microscopes equipped with DC350F and DC300 CCD on bright field, rhodamine, fluorescein or UV channels. Only representative images were used for statistical analysis.

BrdU labeling and flow cytometry

To label the proliferating progenitors in retina, newborn mice at P2 were injected with 50 μg of BrdU/g of body weight by percutaneous intravenous injection (54). The progenitors were labeled at S-phase. During the process of INM, the localization of progenitors was examined on retina sections by changing the BrdU exposure time.

The cell cycle distribution of progenitors was analyzed following a previous protocol with minor modifications (55). Briefly, the retinas were dissociated with 0.06% trypsin + EDTA solution in PBS for 5 min at 37°C and then treated with 60 μg of DNase I. The dissociated cells were harvested and fixed with 0.25% paraformaldehyde in PBS for 10 min.

After incubation in 2 N HCl for 30 min and neutralization by borate solution, the cells were stained with anti-BrdU antibody (eBioscience, 11-6071-73, 1:100). Flow cytometry was performed using the FACSCalibur flow cytometer (BD Biosciences) and analyzed using CellQuest (BD Biosciences) and FlowJo (Tree Star) software.

Mouse ERG

In general, 10- to-12-week-old female mice were allowed to dark-adapt overnight. These mice were then anesthetized with intraperitoneal injection of ketamine (200 mg/kg) and xylazine (10 mg/kg) mixtures. Three needle electrodes were pierced into the mouse tail and both sides of the shoulder skin, respectively, and two other cornea electrodes specific for mice were placed on the mouse corneas. The ERG responses were recorded by Electroretinograms System (RETIport32, Roland consult, Germany).

Statistical analysis

Comparisons between groups were made by an unpaired two-tailed Student's *t*-test. The *P*-value was calculated based on the comparison with controls. Data are reported as means ± standard errors for triplicate sections of retina from at least three mice per group.

co-IP and immunoblot analysis

co-IP and immunoblot analyses with antibodies against dynein IC, p150 and KIF5B were done according to the procedures described previously (14). Briefly, the retinas were homogenized in TNP buffer [50 mM Tris–HCl (pH 7.4), 150 mM NaCl and 0.3% NP-40] and extracted for 30 min on ice. After centrifugation (13 000*g* for 10–15 min), the supernatant was mixed with the antibody or control IgG and rotated end-over-end for 6 h at 4°C. Aliquots were further centrifuged and then incubated with protein A agarose overnight at 4°C. The beads were then collected at 1000*g* and were washed thoroughly in TNP buffer four times. Finally, the beads were boiled in the loading buffer and were subjected to SDS–PAGE (5–10%), followed by immunoblot analyses with enhanced chemiluminescence detection according to the manufacturer's instructions (Pierce and Santa Cruz).

SUPPLEMENTARY MATERIAL

Supplementary Material is available at *HMG* online.

ACKNOWLEDGEMENTS

We thank Xiaobing Yuan (Chinese Academy of Sciences) and Larry A. Donoso (Wills Eye Institute) for generously providing antibodies; Rongrui Zhao and Xiaoping Huang for kindly helping with mice; Beibei Ying, Xiaohui Wu, Kejing Deng, Lin Sun, Wufan Tao and other members of the IDM for assistance and discussions; and Dr Rosanne M. Yetemian (USC) for her technical expertise and scientific discussions.

Conflict of Interest statement. None declared.

FUNDING

This work was supported by grants from the National Basic Research Program of China (NBRP 973 project 2006CB806700), National Hi-Tech Research and Development Program of China (863 project 2007AA022101), 211 and 985 projects of the Chinese Ministry of Education. M.Z. and G.X. are supported by grants from NBRP 973 project (2007CB512205), National Nature Science Foundation of China (30971650 and 30872825), Shanghai Subject Chief Scientist Program (09XD1400900) and Shanghai Pujiang Program (09PJ1402400). C.M.C. is the Mary D. Allen Chair in Vision Research, DEI, is supported by grants from the NIH [EY015851 and EY03040 (DEI core grant)] and is a recipient of a Senior Scientific Investigator award from Research to Prevent Blindness.

REFERENCES

1. Turner, D.L. and Cepko, C.L. (1987) A common progenitor for neurons and glia persists in rat retina late in development. *Nature*, **328**, 131–136.
2. Blanks, J.C., Adinolfi, A.M. and Lolley, R.N. (1974) Synaptogenesis in the photoreceptor terminal of the mouse retina. *J. Comp. Neurol.*, **156**, 81–93.
3. Hinds, J.W. and Hinds, P.L. (1979) Differentiation of photoreceptors and horizontal cells in the embryonic mouse retina: an electron microscopic, serial section analysis. *J. Comp. Neurol.*, **187**, 495–511.
4. Young, R.W. (1984) Cell death during differentiation of the retina in the mouse. *J. Comp. Neurol.*, **229**, 362–373.
5. Young, R.W. (1985) Cell differentiation in the retina of the mouse. *Anat. Rec.*, **212**, 199–205.
6. Young, R.W. (1985) Cell proliferation during postnatal development of the retina in the mouse. *Brain Res.*, **353**, 229–239.
7. Baye, L.M. and Link, B.A. (2008) Nuclear migration during retinal development. *Brain Res.*, **1192**, 29–36.
8. Frade, J.M. (2002) Interkinetic nuclear movement in the vertebrate neuroepithelium: encounters with an old acquaintance. *Prog. Brain Res.*, **136**, 67–71.
9. Rich, K.A., Zhan, Y. and Blanks, J.C. (1997) Migration and synaptogenesis of cone photoreceptors in the developing mouse retina. *J. Comp. Neurol.*, **388**, 47–63.
10. Szel, A., Rohlich, P., Caffe, A.R., Juliusson, B., Aguirre, G. and Van Veen, T. (1992) Unique topographic separation of two spectral classes of cones in the mouse retina. *J. Comp. Neurol.*, **325**, 327–342.
11. Soucy, E., Wang, Y., Nirenberg, S., Nathans, J. and Meister, M. (1998) A novel signaling pathway from rod photoreceptors to ganglion cells in mammalian retina. *Neuron*, **21**, 481–493.
12. Carter-Dawson, L.D. and LaVail, M.M. (1979) Rods and cones in the mouse retina. I. Structural analysis using light and electron microscopy. *J. Comp. Neurol.*, **188**, 245–262.
13. Starr, D.A. and Han, M. (2002) Role of ANC-1 in tethering nuclei to the actin cytoskeleton. *Science*, **298**, 406–409.
14. Zhang, X., Lei, K., Yuan, X., Wu, X., Zhuang, Y., Xu, T., Xu, R. and Han, M. (2009) SUN1/2 and Syne/Nesprin-1/2 complexes connect centrosome to the nucleus during neurogenesis and neuronal migration in mice. *Neuron*, **64**, 173–187.
15. Minn, I.L., Rolls, M.M., Hanna-Rose, W. and Malone, C.J. (2009) SUN-1 and ZYG-12, mediators of centrosome-nucleus attachment, are a functional SUN/KASH pair in *Caenorhabditis elegans*. *Mol. Biol. Cell*, **20**, 4586–4595.
16. Lei, K., Zhang, X., Ding, X., Guo, X., Chen, M., Zhu, B., Xu, T., Zhuang, Y., Xu, R. and Han, M. (2009) SUN1 and SUN2 play critical but partially redundant roles in anchoring nuclei in skeletal muscle cells in mice. *Proc. Natl Acad. Sci. USA*, **106**, 10207–10212.
17. Kracklauer, M.P., Banks, S.M., Xie, X., Wu, Y. and Fischer, J.A. (2007) *Drosophila* klaroid encodes a SUN domain protein required for Klarsicht localization to the nuclear envelope and nuclear migration in the eye. *Fly (Austin)*, **1**, 75–85.

18. McGee, M.D., Rillo, R., Anderson, A.S. and Starr, D.A. (2006) UNC-83 is a KASH protein required for nuclear migration and is recruited to the outer nuclear membrane by a physical interaction with the SUN protein UNC-84. *Mol. Biol. Cell*, **17**, 1790–1801.
19. Haque, F., Lloyd, D.J., Smallwood, D.T., Dent, C.L., Shanahan, C.M., Fry, A.M., Trembath, R.C. and Shackleton, S. (2006) SUN1 interacts with nuclear lamin A and cytoplasmic nesprins to provide a physical connection between the nuclear lamina and the cytoskeleton. *Mol. Cell. Biol.*, **26**, 3738–3751.
20. Crisp, M., Liu, Q., Roux, K., Rattner, J.B., Shanahan, C., Burke, B., Stahl, P.D. and Hodzic, D. (2006) Coupling of the nucleus and cytoplasm: role of the LINC complex. *J. Cell Biol.*, **172**, 41–53.
21. Padmakumar, V.C., Libotte, T., Lu, W., Zaim, H., Abraham, S., Noegel, A.A., Gotzmann, J., Foisner, R. and Karakesisoglou, I. (2005) The inner nuclear membrane protein Sun1 mediates the anchorage of Nesprin-2 to the nuclear envelope. *J. Cell Sci.*, **118**, 3419–3430.
22. Malone, C.J., Misner, L., Le Bot, N., Tsai, M.C., Campbell, J.M., Ahringer, J. and White, J.G. (2003) The *C. elegans* hook protein, ZYG-12, mediates the essential attachment between the centrosome and nucleus. *Cell*, **115**, 825–836.
23. Starr, D.A., Hermann, G.J., Malone, C.J., Fixsen, W., Priess, J.R., Horvitz, H.R. and Han, M. (2001) unc-83 encodes a novel component of the nuclear envelope and is essential for proper nuclear migration. *Development*, **128**, 5039–5050.
24. Patterson, K., Molofsky, A.B., Robinson, C., Acosta, S., Cater, C. and Fischer, J.A. (2004) The functions of Klarsicht and nuclear lamin in developmentally regulated nuclear migrations of photoreceptor cells in the *Drosophila* eye. *Mol. Biol. Cell*, **15**, 600–610.
25. Del Bene, F., Wehman, A.M., Link, B.A. and Baier, H. (2008) Regulation of neurogenesis by interkinetic nuclear migration through an apical-basal notch gradient. *Cell*, **134**, 1055–1065.
26. Tsujikawa, M., Omori, Y., Biyanwila, J. and Malicki, J. (2007) Mechanism of positioning the cell nucleus in vertebrate photoreceptors. *Proc. Natl Acad. Sci. USA*, **104**, 14819–14824.
27. Zhang, J., Felder, A., Liu, Y., Guo, L.T., Lange, S., Dalton, N.D., Gu, Y., Peterson, K.L., Mizisin, A.P., Shelton, G.D. *et al.* (2010) Nesprin 1 is critical for nuclear positioning and anchorage. *Hum. Mol. Genet.*, **19**, 329–341.
28. Puckelwartz, M.J., Kessler, E., Zhang, Y., Hodzic, D., Randles, K.N., Morris, G., Earley, J.U., Hadhazy, M., Holaska, J.M., Mewborn, S.K. *et al.* (2009) Disruption of nesprin-1 produces an Emery Dreifuss muscular dystrophy-like phenotype in mice. *Hum. Mol. Genet.*, **18**, 607–620.
29. Chi, Y.H., Cheng, L.I., Myers, T., Ward, J.M., Williams, E., Su, Q., Faucette, L., Wang, J.Y. and Jeang, K.T. (2009) Requirement for Sun1 in the expression of meiotic reproductive genes and piRNA. *Development*, **136**, 965–973.
30. Ding, X., Xu, R., Yu, J., Xu, T., Zhuang, Y. and Han, M. (2007) SUN1 is required for telomere attachment to nuclear envelope and gametogenesis in mice. *Dev. Cell*, **12**, 863–872.
31. Zhang, X., Xu, R., Zhu, B., Yang, X., Ding, X., Duan, S., Xu, T., Zhuang, Y. and Han, M. (2007) Syne-1 and Syne-2 play crucial roles in myonuclear anchorage and motor neuron innervation. *Development*, **134**, 901–908.
32. Brzezinski, J.A. IV, Brown, N.L., Tanikawa, A., Bush, R.A., Sieving, P.A., Vitaterna, M.H., Takahashi, J.S. and Glaser, T. (2005) Loss of circadian photoentrainment and abnormal retinal electrophysiology in Math5 mutant mice. *Invest. Ophthalmol. Vis. Sci.*, **46**, 2540–2551.
33. Nikonov, S.S., Brown, B.M., Davis, J.A., Zuniga, F.I., Bragin, A., Pugh, E.N. Jr and Craft, C.M. (2008) Mouse cones require an arrestin for normal inactivation of phototransduction. *Neuron*, **59**, 462–474.
34. Brown, B.M., Ramirez, T., Rife, L. and Craft, C.M. (2010) Visual Arrestin 1 contributes to cone photoreceptor survival and light adaptation. *Invest. Ophthalmol. Vis. Sci.*, **51**, 2372–2380.
35. Zhu, X., Li, A., Brown, B., Weiss, E.R., Osawa, S. and Craft, C.M. (2002) Mouse cone arrestin expression pattern: light induced translocation in cone photoreceptors. *Mol. Vis.*, **8**, 462–471.
36. Kandel, E.R., Schwartz, J.H. and Jessell, T.M. (2000) *Principles of Neural Science*, 4th edn. McGraw-Hill, New York, pp. 507–513.
37. Pugh, E.N. Jr, Falsini, B. and Lyubarsky, A.L. (1998) The origin of the major rod- and cone-driven components of the rodent electroretinogram, and the effect of age and light rearing history on the magnitudes of these components. In Williams, T.P. and Thistle, A.B. (eds), *Photostasis and Related Topics*. Plenum, New York, pp. 93–128.
38. King, S.J. and Schroer, T.A. (2000) Dynactin increases the processivity of the cytoplasmic dynein motor. *Nat. Cell Biol.*, **2**, 20–24.
39. Fan, S.S. and Ready, D.F. (1997) Glued participates in distinct microtubule-based activities in *Drosophila* eye development. *Development*, **124**, 1497–1507.
40. Whited, J.L., Cassell, A., Brouillette, M. and Garrity, P.A. (2004) Dynactin is required to maintain nuclear position within postmitotic *Drosophila* photoreceptor neurons. *Development*, **131**, 4677–4686.
41. Starr, D.A. (2009) A nuclear-envelope bridge positions nuclei and moves chromosomes. *J. Cell Sci.*, **122**, 577–586.
42. Fridolfsson, H.N., Ly, N., Meyerzon, M. and Starr, D.A. (2010) UNC-83 coordinates kinesin-1 and dynein activities at the nuclear envelope during nuclear migration. *Dev. Biol.*, **338**, 237–250.
43. Roux, K.J., Crisp, M.L., Liu, Q., Kim, D., Kozlov, S., Stewart, C.L. and Burke, B. (2009) Nesprin 4 is an outer nuclear membrane protein that can induce kinesin-mediated cell polarization. *Proc. Natl Acad. Sci. USA*, **106**, 2194–2199.
44. Apel, E.D., Lewis, R.M., Grady, R.M. and Sanes, J.R. (2000) Syne-1, a dystrophin- and Klarsicht-related protein associated with synaptic nuclei at the neuromuscular junction. *J. Biol. Chem.*, **275**, 31986–31995.
45. Puckelwartz, M.J., Kessler, E.J., Kim, G., Dewitt, M.M., Zhang, Y., Earley, J.U., Depreux, F.F., Holaska, J., Mewborn, S.K., Pytel, P. *et al.* (2010) Nesprin-1 mutations in human and murine cardiomyopathy. *J. Mol. Cell Cardiol.*, **48**, 600–608.
46. Luke, Y., Zaim, H., Karakesisoglou, I., Jaeger, V.M., Sellin, L., Lu, W., Schneider, M., Neumann, S., Beijer, A., Munck, M. *et al.* (2008) Nesprin-2 Giant (NUANCE) maintains nuclear envelope architecture and composition in skin. *J. Cell Sci.*, **121**, 1887–1898.
47. Zhen, Y.Y., Libotte, T., Munck, M., Noegel, A.A. and Korenbaum, E. (2002) NUANCE, a giant protein connecting the nucleus and actin cytoskeleton. *J. Cell Sci.*, **115**, 3207–3222.
48. Ayala, R., Shu, T. and Tsai, L.H. (2007) Trekking across the brain: the journey of neuronal migration. *Cell*, **128**, 29–43.
49. Tsai, J.W., Lian, W.N., Kemal, S., Kriegstein, A.R. and Vallee, R.B. (2010) Kinesin 3 and cytoplasmic dynein mediate interkinetic nuclear migration in neural stem cells. *Nat. Neurosci.*, **13**, 1463–1471.
50. Fridolfsson, H.N. and Starr, D.A. (2010) Kinesin-1 and dynein at the nuclear envelope mediate the bidirectional migrations of nuclei. *J. Cell Biol.*, **191**, 115–128.
51. Vallee, R.B., Seale, G.E. and Tsai, J.W. (2009) Emerging roles for myosin II and cytoplasmic dynein in migrating neurons and growth cones. *Trends Cell Biol.*, **19**, 347–355.
52. Schenk, J., Wilsch-Brauninger, M., Calegari, F. and Huttner, W.B. (2009) Myosin II is required for interkinetic nuclear migration of neural progenitors. *Proc. Natl Acad. Sci. USA*, **106**, 16487–16492.
53. Norden, C., Young, S., Link, B.A. and Harris, W.A. (2009) Actomyosin is the main driver of interkinetic nuclear migration in the retina. *Cell*, **138**, 1195–1208.
54. Sands, M.S. and Barker, J.E. (1999) Percutaneous intravenous injection in neonatal mice. *Lab Anim. Sci.*, **49**, 328–330.
55. Sakagami, K., Gan, L. and Yang, X.J. (2009) Distinct effects of Hedgehog signaling on neuronal fate specification and cell cycle progression in the embryonic mouse retina. *J. Neurosci.*, **29**, 6932–6944.